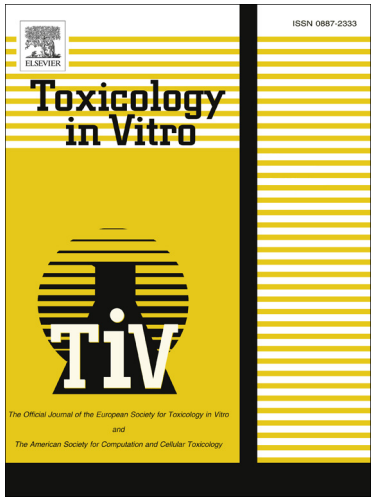

Novel *o*-naphthoquinones induce apoptosis of EL-4 T lymphoma cells through the increase of reactive oxygen species

María Emilia Di Rosso, María Laura Barreiro Arcos, Igal Elingold, Helena A. Sterle, Sabrina Baptista Ferreira, Vitor F. Ferreira, Mónica Galleano, Graciela Cremaschi, Marta Dubin

PII: S0887-2333(13)00191-4
DOI: http://dx.doi.org/10.1016/j.tiv.2013.08.002
Reference: TIV 3159

To appear in: *Toxicology in Vitro*

Received Date: 19 April 2013
Accepted Date: 1 August 2013

Please cite this article as: Rosso, a.E.D., Arcos, a.L.B., Elingold, I., Sterle, H.A., Ferreira, S.B., Ferreira, V.F., Galleano, M., Cremaschi, G., Dubin, M., Novel *o*-naphthoquinones induce apoptosis of EL-4 T lymphoma cells through the increase of reactive oxygen species, *Toxicology in Vitro* (2013), doi: http://dx.doi.org/10.1016/j.tiv.2013.08.002

Novel *o*-naphthoquinones induce apoptosis of EL-4 T lymphoma cells through the increase of reactive oxygen species

María Emilia Di Rosso[a], María Laura Barreiro Arcos[b], Igal Elingold[a], Helena A. Sterle[b], Sabrina Baptista Ferreira[c], Vitor F. Ferreira[d], Mónica Galleano[e], Graciela Cremaschi[b], Marta Dubin[a*]

M.E. Di Rosso and M.L. Barreiro Arcos contributed equally to this paper.

[a] Centro de Estudios Farmacológicos y Botánicos (CEFYBO), Facultad de Medicina, Universidad de Buenos Aires-CONICET, Paraguay 2155, piso 16, C1121ABG, Buenos Aires, Argentina.

[b] Instituto de Investigaciones Biomédicas, Facultad de Ciencias Médicas, Pontificia Universidad Católica Argentina (UCA), Av. Alicia Moreau de Justo 1300, C1107AAZ, Buenos Aires, Argentina.

[c] Departamento de Química Orgânica, Instituto de Química, Universidade Federal do Rio de Janeiro, Av. Athos da Silveira Ramos 149, 21941-909, Cidade Universitária, Rio de Janeiro, Brazil.

[d] Departamento de Química Orgânica, Instituto de Química, UFF, Outeiro São João Batista s/n, 24020-141, Campus do Valonguinho, Niterói, Brazil.

[e] Fisicoquímica-Instituto de Bioquímica y Medicina Molecular (IBIMOL), Facultad de Farmacia y Bioquímica, UBA-CONICET, Junín 956, C1113AAD, Buenos Aires, Argentina.

*Corresponding author:
Marta Dubin PhD.
Tel: 54 114508-3680x107
Fax: 54 114508-3680
E-mail: dubinmarta@yahoo.com.ar

ABSTRACT

Novel β-lapachone analogs 2-phenyl-3,4-dihydro-2*H*-benzo[*h*]chromene-5,6-dione (NQ1), 2-p-tolyl-3,4-dihydro-2*H*-benzo[*h*]chromene-5,6-dione (NQ3) and 2-methyl-2-phenyl-3,4-dihydro-2H-benzo[*h*]chromene-5,6-dione (NQ7), which have trypanocidal activity, were assayed for cytotoxic effects on murine EL-4 T lymphoma cells. The NQs inhibited the proliferation of EL-4 cells at concentrations above 1 μM. Nuclear staining of the EL-4 cells revealed chromatin condensation and a nuclear morphology compatible with the induction of apoptosis. Flow cytometry assays with annexin V-FITC and propidium iodide confirmed the cell death by apoptosis. Using electron paramagnetic resonance (EPR), a semiquinone radical was detected in EL-4 cells treated with NQs. In addition, a decrease in the GSH level in parallel with reactive oxygen species (ROS) production was observed. Preincubation with n-acetyl-l-cysteine (NAC) was able to reverse the inhibitory effects of the NQs on cell proliferation, indicating that ROS generation is involved in NQ-induced apoptosis. In addition, the NQs induced a decrease in the mitochondrial membrane potential and increased the proteolytic activation of caspases 9 and 3 and the cleavage of Poly (ADP-Ribose) Polymerase (PARP). In conclusion, these results indicate that redox cycling is induced by the NQs in the EL-4 cell line, with the generation of ROS and other free radicals that could inhibit cellular proliferation as a result of the induction of the intrinsic apoptosis pathway.

Keywords : *o*-naphthoquinones; oxidative stress; apoptosis.

Abbreviations list

NQ1: 2-phenyl-3,4-dihydro-2*H*-benzo[*h*]chromene-5,6-dione; NQ3: 2-p-tolyl-3,4-dihydro-2*H*-benzo[*h*]chromene-5,6-dione; NQ7: 2-methyl-2-phenyl-3,4-dihydro-2H-benzo[*h*]chromene-5,6-dione; DMFA: *N,N*-dimethyl-formamide; AO: acridine orange; EB: ethidium bromide; PI: propidium iodide; EPR: electron paramagnetic resonance; ROS: reactive oxygen species; H2DCF-DA: 2,7-dichlorodihydrofluorescein diacetate; DTNB: 5,5´-dithiobis-2-nitrobenzoic acid; TCA: trichloroacetic acid; TNB: 2-nitro-5-thiobenzoic acid; NAC: n-acetyl-l-cysteine; Rho-123: rhodamine-123; PARP: Poly (ADP-Ribose) Polymerase; PTP: permeability transition pore; MMP: mitochondrial membrane potential.

1. INTRODUCTION

Quinones are considered privileged structures in medicinal chemistry because of their biological activities and structural properties (Bolton et al., 2000; Costantino and Barlocco, 2006). Indeed, several quinones, such as doxorubicin, mitomycin, and mitoxantrone, are medicines that are still used clinically for the treatment of solid cancers (Edmonson et al., 1993). Among quinones, naphthoquinones are especially important due to their biological activities and structural properties (Costantino and Barlocco, 2006). The biological profiles of these molecules are based on their *ortho*- or *para*-quinoid moiety. This group generally accepts one and/or two electrons to form the corresponding radical species, and the driving force behind this redox property is the formation of a fully aromatic system (Asche, 2005; Hillard et al., 2008). In biological systems, naphthoquinones are reduced to semiquinone radicals through two different pathways (de Witte et al., 2004; Elingold et al., 2009; Fernandez Villamil et al., 2004; Thor et al., 1982). The one-electron reduction and direct formation of semiquinone is catalyzed primarily by microsomal NADPH-cytochrome P450 reductase. The two-electron reduction is catalyzed by the cytosolic flavoprotein DT-diaphorase (NADPH (quinone acceptor) oxidoreductase NQO1) and generates hydroquinone, which can be reoxidized and indirectly form the semiquinone (Cadenas, 1995; dos Santos et al., 2004). This radical is capable of transferring electrons to molecular oxygen, thereby returning to its original quinoidal structure and generating a superoxide anion radical ($O_2^{\bullet-}$). Superoxide dismutases to hydrogen peroxide (H_2O_2), and then the hydroxyl radical ($OH^{\bullet}$) can be formed (Boveris et al., 1978a; Molina Portela et al., 1996; Molina Portela and Stoppani, 1996). These highly reactive oxygen species (ROS) can cause damage to DNA, lipids, and proteins (Brunmark and Cadenas, 1989; Valko et al., 2007). A great number of physiological functions are controlled by redox-responsive pathways (Droge, 2002). It has been reported that the induction of apoptosis via the mitochondrial pathway can be mediated by an increase in the ROS level (Hampton et al., 1998; Kroemer et al., 2007; Seshadri et al., 2011; Xu et al., 2012; Xu et al., 2010).

Among naphthoquinones, *o*-naphthoquinones are interesting because of their electronic structure, which makes them more active than *p*-naphthoquinones against trypanosomatids and human cancer cell lines (Boveris et al., 1978a; Kongkathip et al., 2003; Lopes et al., 1978; Molina Portela et al., 1996). The natural *o*-naphthoquinone β-lapachone has been

intensely investigated not only due to its trypanocidal activity but also for clinical use in cancer therapy (Goijman and Stoppani, 1985; Pardee et al., 2002). The studies on β-lapachone focused on cancer chemotherapy pointed to topoisomerases I and II as its biochemical targets in the induction of apoptosis (Li et al., 1995). The cytotoxicity of β-lapachone prompted the synthesis of a number of *o*-naphthoquinones to establish the structural requirements for optimal therapeutic use. Ferreira et al. (2011) synthesized new derivatives from β-lapachone. Among these compounds are 2-phenyl-3,4-dihydro-2*H*-benzo[*h*]chromene-5,6-dione (NQ1), 2-*p*-tolyl-3,4-dihydro-2*H*-benzo[*h*]chromene-5,6-dione (NQ3) and 2-methyl-2-phenyl-3,4-dihydro-2H-benzo[*h*]chromene-5,6-dione (NQ7) (Figure 1), which were only investigated against bloodstream trypomastigotes of *Trypanosoma cruzi*, the etiologic agent of Chagas disease, and proved to be more active than β-lapachone (Ferreira et al., 2011).

In the present study, we investigated the cytotoxic effects of NQs on EL-4 murine lymphoma cells and analyzed the mechanisms of action involved. To better understand the mechanism underlying the cytotoxicity of these compounds, studies involving the analysis of changes in nuclear morphology, the permeability of membranes, phosphatidyl serine externalization, semiquinone formation, ROS generation and mitochondrial membrane potential were performed. The activation of the proteolytic cascade of enzymes involved in apoptosis, such as caspase 9 and caspase 3, and the inactivation by cleavage of poly(ADP-ribose) polymerase (PARP) were investigated to analyze the intracellular signals involved. Our results indicate that the production of ROS and the semiquinone radical formation induced by NQ redox cycling may induce mitochondrial (intrinsic) pathway-dependent apoptosis involving the proteolytic activation of caspases 9 and 3 and PARP cleavage.

2. MATERIALS AND METHODS

2.1. Chemicals

The NQs used in this study were synthesized as previously described (Ferreira et al., 2011). The β-lapachone analogs were synthesized by the Knoevenagel condensation of 2-hydroxy-1,4-naphthoquinone with paraformaldehyde or arylaldehydes, followed by a

hetero-Diels-Alder reaction with substituted styrenes in aqueous ethanol media, generating different β-lapachone analogs. The structures of the synthesized compounds were confirmed using spectroscopic techniques, such as 1H and 13C NMR, infrared spectroscopy, and HRMS (ESI), and our data are consistent with those reported previously.

The chemical structures of NQs are shown in Figure 1. These compounds were provided as lyophilized powders and were diluted in *N*,*N*-dimethyl-formamide (DMFA). Controls received the same volume of solvent, whose concentration never exceeded 0.5% (v/v). RPMI 1640 cell culture medium, fetal calf serum, glutamine, penicillin and streptomycin were purchased from Gibco (USA). [^{3}H]-Thymidine was purchased from New England Nuclear, Perkin Elmer Inc, Boston, MA, USA. HCl, NaCl, $CaCl_2$, NaOH and KCl were provided by Merck Química Argentina S.A. (Buenos Aires, Argentina). *N*-Acetylcysteine (NAC), trypan blue, fetal calf serum (FCS), fetal bovine serum (FBS), phosphate-buffered saline (PBS), Hoechst 33258, acridine orange (AO), ethidium bromide (EB), DMFA, HEPES, annexin V-FITC, propidium iodide (PI), KH_2PO_4, K_2HPO_4, NADPH, 2,7-dichlorodihydrofluorescein diacetate (H2DCF-DA), trichloroacetic acid (TCA), GSH, 5,5′-dithiobis(2-nitrobenzoic acid) (DTNB), glutathione reductase, 4-vinylpyridine, rhodamine 123 (Rho-123), Trizma base, [ethylenebis(oxyethylenenitrilo)]tetraacetic acid (EGTA), NP-40, NaF, Na_3VO_4, sodium deoxycholate, phenylmethylsulfonyl fluoride, aprotinin, pepstatin, leupeptin, SDS, glycerol, bromophenol blue, 2-mercaptoethanol, acrylamide, N',N'-methylene bisacrylamide and Tween were acquired from Sigma Chemical Co. (St. Louis, Mo, USA). Rabbit anti-active caspase 9 and rabbit anti-active caspase 3 antibodies were purchased from Abcam^R (USA). Mouse anti-cleaved PARP was acquired from BD Biosciences (San Jose, CA, USA). The rabbit anti- -actin antibody was purchased from Santa Cruz Biotechnology, Inc (Santa Cruz, CA, USA). Anti-rabbit or anti-mouse secondary antibodies coupled to horseradish peroxidase were acquired from Signaling Technology, Inc. (Beverly, MA, USA). All other chemicals used in this study were of analytical grade.

2.2. Cell suspensions and culture conditions

EL-4 mouse T lymphoma cells (American Type Culture Collection, ATCC, Manassas, VA, USA) were cultured at an optimal concentration of $1–5\times10^5$ cells/ml in RPMI 1640

medium supplemented with 10% FCS, 2 mM glutamine, 100 g/ml of penicillin and 150 g/ml of streptomycin. The culture medium was changed every day after the cells had reached the exponential growth phase. The cells were kept in T-25 culture flasks (Corning, NY) at 37 ºC with a 5% CO_2 atmosphere.

2.3. Proliferation assays and viability studies

EL-4 cells were cultured for 24 h in the absence (control) or presence of increasing concentrations of the NQs, and proliferation was evaluated in 96-well microplates (Nunc^{TM}) using a pulse of [^{3}H]thymidine ([^{3}H]-TdR, 20 Ci/mmol) 16 h before the end of the incubation period. At the end of culture incubation period, the cells were harvested, and the amount of [^{3}H]-TdR incorporated to the DNA was quantified using a liquid scintillation counter (Barreiro Arcos et al., 2003). In the experiments involving NAC treatment, EL-4 cells were incubated with NAC for 18 h prior to culturing the cells under the conditions described previously (Donadelli et al., 2006). The results were expressed as the dpm values for the NQ-treated cells minus the dpm values for the control (cells treated with vehicle). Cytotoxic activity expressed by IC50±SE (M) of compounds for EL-4 cell line was obtained by nonlinear regression from three independent experiments. Cell viability was determined by trypan blue exclusion. Viability is expressed as the percentage of living cells and was calculated as follows: [number of viable cells / number of total cells] × 100.

2.4. Chromatin condensation assay with Hoechst 33258 staining

T lymphoma cells were cultured in RPMI 1640 medium supplemented with FBS in the absence or presence of NQs for the indicated times, and then the nuclear morphology of the cells was examined. Briefly, the cells were washed and resuspended in PBS at a concentration of $1x10^6$ cells/ml, plated onto slides and fixed with ethanol. A nuclear staining solution containing 0.01 mg/ml Hoechst 33258 was added for 10 min. The cells were washed three times with PBS, and the nuclear morphology was then examined using a fluorescence microscope (Nikon Diaphou; Nikon Inc., Melville, NY).

2.5. Acridine orange staining

The presence of apoptotic morphology was analyzed by double staining with acridine orange and ethidium bromide (AO/EB). EL-4 cells were plated at a density of $1x10^6$ cells/ml and were incubated with NQs at 5 μM for different times. Then, the cells were washed twice and resuspended in 300 l of PBS. Ten microliters of a fluorescent dye mixture containing AO and EB (both 100 μg/ml) were added to the cells for 10 min. Freshly stained cell suspensions were dropped onto glass slides and covered by coverslips. The slides were observed under a UV-fluorescence microscope (Nikon Diaphou; Nikon Inc., Melville, NY) at a magnification of 1000x (Coligan, 1995).

2.6. Quantification of apoptosis by flow cytometry

EL-4 cells were incubated in the absence or presence of NQs (5 μM) for different times. Then, $1x10^6$ cells were washed once with PBS, resuspended in 0.5 ml of staining buffer (10 mM HEPES/NaOH, pH 7.5; 0.14 M NaCl; 2.5 mM $CaCl_2$) and then incubated for 15 min in the dark with 5 μl of annexin V-FITC (1 mg/ml) and 10 μl of propidium iodide (PI, 1 mg/ml) (Vermes et al., 1995). The labeled cells were analyzed by flow cytometry (FACSCalibur, Becton Dickinson Biosciences), and the fluorescence intensities at 580 nm (PI) and 520 nm (annexin V-FITC) were quantified. The data were analyzed with WinMDI 2.8 and were expressed as the percentage of cells in each subpopulation (unstained, stained with PI, stained with FITC or stained with both) with respect to the total number of cells analyzed (Walsh et al., 1998).

2.7. Analysis of free radical semiquinones

Semiquinone radicals were detected by electron paramagnetic resonance (EPR) at room temperature under anaerobic conditions as previously described (Elingold et al., 2009). Briefly, EL-4 cells ($2x10^6$) were incubated with NQs (5 mM) in potassium phosphate buffer (0.1 M, pH 7.4) and NADPH (20 mM) in a final volume of 0.15 ml. The time elapsed between the preparation of the reaction mixture and the recording of the EPR spectra was approximately 5 min, and this period was considered as the incubation time. EPR measurements were performed on a Bruker BioSpin EMX Plus spectrometer (Bruker, Karlsruhe, Germany). The instrumental conditions were as follows: microwave

power, 20 mW; microwave frequency, 9.75 GHz; modulation amplitude, 1 G; modulation frequency, 50 kHz; time constant, 164 ms; and centerfield, 3490 G.

2.8. Reactive oxygen species (ROS) measurement

The intracellular level of reactive oxygen species (ROS) was determined using the fluorescent probe 2,7-dichlorodihydrofluorescein diacetate (H2DCF-DA) (LeBel et al., 1992). EL-4 cells were cultured in the absence or presence of the NQs (5 M). After the appropriate culture duration, $1x10^6$ cells were washed and resuspended in 1 ml of PBS. Cells were incubated with 10 μM DCF-DA for 20 min at 37ºC, and the fluorescence was quantified using a FACSCalibur flow cytometer (Becton Dickinson Biosciences) at 480 nm. In the experiments involving NAC treatment, EL-4 cells were incubated with NAC (12.5 mM) for 18 h prior to culturing the cells under the conditions described previously. The data were analyzed using WinMDI 2.8.

2.9 Determination of the intracellular glutathione levels

The glutathione levels were determined using the method of Griffith (Griffith, 1980). Briefly, EL-4 cells were cultured in the absence or presence of NQs for different times. Then, cells were washed, resuspended in PBS and pelleted at 1000 x g for 10 min. The cell pellets were resuspended in 200 μl of TCA (0.5%) and frozen at –20°C. Then, the pellets were thawed and centrifuged to remove the cellular debris. The supernatants were used to quantify the total glutathione and GSSG levels. The total glutathione level was determined using an enzyme recycling procedure, in which the GSH is oxidized by 5,5´-dithiobis(2-nitrobenzoic acid) (DTNB) and reduced by NADPH in the presence of glutathione reductase. The formation of 2-nitro-5-thiobenzoic acid (TNB) was monitored at 412 nm. In the experiments involving NAC treatment, EL-4 cells were incubated with NAC for 18 h prior to culturing the cells under the conditions described previously. The total glutathione values of the sample were extrapolated to a standard curve of known concentrations of GSH. For GSSG quantification, samples were preincubated with 4-vinylpyridine. The level of reduced glutathione was determined by the formula GSH= [total glutathione–GSSG].

2.10 Determination of the mitochondrial membrane potential

EL-4 cells were cultured in the absence or presence of NQs for 3.5 h, and aliquots of the cell cultures ($1x10^6$ cells/ml) were incubated with 1 μM rhodamine 123 (Rho-123) for 30 min. The cells were then centrifuged and resuspended in PBS. Changes in the mitochondrial membrane potential were detected by flow cytometry using a FACSCalibur flow cytometer.

2.11 Immunoblot analysis

EL-4 cells were cultured in the absence or presence of NQs (5 M) for different times. Then, the cells were lysed for 30 min at 4°C in lysis buffer (50 mmol/L Tris-HCl, 150 mmol/L NaCl, 1 mmol/L EGTA, 1% NP-40, 1 mmol/L NaF, 1 mmol/L Na_3VO_4, 0.25% sodium deoxycholate, 1 μmol/L phenylmethylsulfonyl fluoride, 10 μg/mL aprotinin, 10 μmol/L pepstatin and 10 μmol/L leupeptin). After centrifugation (14,000 g, 15 min, 4°C), the whole-cell protein extracts (50 μg) were mixed with SDS sample buffer (2% SDS, 10% (v/v) glycerol, 62.5 mM Tris–HCl, pH 6.8, 0.2% bromophenol blue and 1% (v/v) 2-mercaptoethanol). Equal amounts of protein were separated by SDS–PAGE on 10% polyacrylamide gels and transferred to PVDF membranes. Nonspecific binding sites on the nitrocellulose membranes were blocked with blocking buffer (5% nonfat dried milk containing 0.1% Tween 20 in 100 mM Tris–HCl, pH 7.5, and 0.9% NaCl) for 1 h. Then, the PVDF membranes were incubated overnight with rabbit anti-active caspase 9, rabbit anti-active caspase 3, mouse anti-cleaved PARP or rabbit anti- -actin antibodies, all of which were used at a dilution of 1:1000. After being washed three times for 10 min with PBS-Tween, the membranes were subsequentially exposed to anti-rabbit or anti-mouse (1:2500) antibodies coupled to horseradish peroxidase for 1 h. After the membranes were washed three times for 10 min with PBS-Tween and once with PBS, an enhanced chemiluminescent system (GE Healthcare Bio-Sciences) was used for detection. The amount of protein loaded in each well was determined using a rabbit anti- actin antibody (1:1000). Densitometry analysis of the bands was performed using Image J software (version 5.1, Silk Scientific Corporation, NIH, Bethesda, MA, USA). The densitometric intensities of the analyzed protein were normalized to those of the corresponding bands for -actin.

2.13. Statistical analysis

The effect of the NQs was calculated by using the corresponding results for the sample containing DMFA as the control value. Data were expressed as mean ± SE of the number of independent experiments indicated in the figure legends, each one performed in triplicate. Analysis of variance (ANOVA) was used to assess the statistical significance of the differences followed by either Dunnett or Tukey post-test. A value of $p < 0.05$ was considered statistically significant. The data were analyzed with the GraphPad Prism version 4.00 (GraphPad Software, San Diego, CA, USA).

3. RESULTS

3.1 Effects of NQs on cell proliferation.

The evaluation of the proliferative activity of cells growing in the presence of different drugs is widely used to investigate the mechanisms of cytotoxicity. To determine the effect of the NQs on the proliferation of EL-4 cells, the amount of [^{3}H]-TdR incorporated into DNA was quantified. Figure 2A shows the proliferation curves of EL-4 cells treated with increasing concentrations of NQs for 24 h. A significant inhibitory effect was observed at concentrations as low as 1 M, and this effect was concentration dependent. Moreover, it was also demonstrated using the trypan blue exclusion method that NQs (5 M) were able to induce a decrease in cell viability in a time-dependent manner, reaching maximum values at 7 h of incubation; this decrease in viability led to an inhibition of EL-4 cell proliferation (Figure 2B). In terms of cytotoxicity, NQ1 (IC50=0.7±0.2 M), NQ3 (IC50=1.1±0.1 M) and NQ7 (IC50=1.0±0.2 M) resulted significantly more active against EL-4 cell line than β-lapachone (IC50=2.0±0.2 M), the naphthoquinoidal precursor.

3.2 Effects of NQs on cell death.

To study the mechanisms by which NQs induce cell death, we determined whether the growth-inhibitory effect of NQs was related to the induction of apoptosis and/or necrosis. To this end, control EL-4 cells and NQ-treated cells (5 μM) were labeled using

AO/EB double staining, and the percentages of viable, apoptotic and necrotic cells were determined by fluorescence microscopy. As shown in Figure 3A, control cells had a normal morphology and green fluorescence, indicating that the cells were viable. The nuclei of the cells were all similar sizes, regularly shaped and evenly stained. Treatment with NQs (5 μM) for 3.5 h increased the number of cells with morphological changes and enhanced the fluorescence. In the groups of cells treated for 7 h, the level of orange cell fluorescence was significantly enhanced, and the chromatin was condensed, indicating that these cells were late apoptotic cells.

To further determine if the cell death mechanism was apoptosis or necrosis, control EL-4 cells and cells treated with NQs (5 μM) for 7 h were labeled with Hoechst 33258 dye, and the nuclear morphology was observed by fluorescence microscopy. Control EL-4 cells had a normal nuclear morphology, similar sizes and regular shapes. However, the NQ-treated cells had a nuclear morphology compatible with apoptosis, with the reduction of the nuclear and cytoplasmic volumes and chromatin condensation (Figure 3B).

The populations of apoptotic (early or late), necrotic and viable cells were quantified using the annexin V-FITC/PI double staining method. As shown in Figure 3C, treatment with NQs (5 μM) decreased cell viability and increased the percentage of cells in the early and late stages of apoptosis in a time-dependent manner. NQ treatment did not induce a significant increase in the percentage of necrotic cells (annexin V-/ IP+). These results are in agreement with the inhibition of cell proliferation observed in the presence of NQs.

3.3 Effects of NQs on semiquinone radical generation.

The NADPH-dependent reduction of NQs in EL-4 cells was confirmed by EPR, indicating that the *o*-seminaphthoquinone radical was formed (Figure 4). At least five lines (a quintuplet) would be expected for these spectra due to the coupling of the free electron with the four aromatic protons C7-C10 in the naphthalene ring. Under our experimental conditions, the quintuplet was clearly observed for NQ7 but was poorly resolved for the other drugs. The apparent splitting constants varied between 1.45 and 1.60 gauss, in agreement with the obtained values for other *o*-seminaphtoquinones

(Kumar et al., 2006). The omission of the NQ or NADPH prevented the appearance of the semiquinone signals. In the absence of cells, there were small signals corresponding to chemical (non-enzymatic) reduction.

3.4 Effects of NQs on ROS production.

The oxidative stress associated with the autoxidation of the semiquinone free radical, which produces the superoxide anion, hydrogen peroxide, and other ROS, has been shown to be related to naphthoquinone's cytotoxicity. To probe the role of ROS generation and increasing oxidative stress as a mechanism associated with NQ toxicity toward EL-4 cells, we measured the intracellular ROS level using the fluorescent probe 2,7 dichlorofluorescein diacetate (DCFDHA). Figures 5A and 5B show a significant increase in ROS accumulation after a 10 min incubation with NQs (5 μM). The highest ROS level was observed after 30 min of incubation. After a longer period of incubation, the ROS level was lower (data not shown).

To further explore the role of oxidative stress in NQ-mediated toxicity, ROS were quantified using the natural antioxidant N-acetyl cysteine (NAC), the most bioavailable precursor of glutathione (Gross et al., 1993). After 18 h incubation with NAC (12.5 mM) a reversal of NQs-induced ROS increasing was observed (Control: 199.18±9.39; NQ1: 201.25±10.51; NQ3: 205.36±9.52; NQ7: 210.51±11.32 MFI) (Supplemental Figure 1).

3.5 Effects of NQs on the cellular redox state.

The increased generation of ROS by NQs likely contributes to oxidative stress, which may ultimately lead to the observed cytotoxicity. The reduced/oxidized glutathione ratio (GSH/GSSG) is used to evaluate the oxidative stress status in biological systems (Gago-Martinez et al., 2004). As seen in Table 1, NQs (5 μM) caused a statistically significant decrease in the GSH/GSSG ratio after a 30 min incubation due to a reduction in the GSH level and an increase in the GSSG level. The pre-incubation of the cells with NAC (12.5 mM) for 18 h before treatment with the NQs (5 μM) for 30 min, restored the GSH/GSSG ratio to the respective control value.

NAC effect was also studied on EL-4 cell proliferation, analyzed by [^{3}H]-TdR incorporation into DNA. The pre-incubation of the cells with NAC (12.5 or 15 mM) for 18 h before treatment with the NQs (2.5 or 5 μM) for 24 h reversed the growth-inhibitory effect of the NQs. This effect was observed in a NAC and NQ concentration-dependent manner (Figure 6). It is worth mentioning that the NAC concentrations used in this experiment had no effects on the proliferation of control cells.

3.6. Effects of NQs on the mitochondrial membrane potential.

To better understand the mechanisms underlying the toxicity of NQs, their ability to interfere with mitochondria was assessed using the fluorescent dye rhodamine 123. A significantly decrease in the MMP was observed in EL-4 cells treated with NQs (5 μM). The lowest MMP values were observed after 3.5 h of incubation (Figure 7). This decrease in the mitochondrial membrane potential could occur due to the opening of the mitochondrial permeability transition pore, which allows the release of proteins such as cytochrome c that trigger the apoptotic pathway (Kroemer et al., 2007).

3.7 Effects of NQs on the proteolytic activation of caspases and PARP cleavage

The involvement of the mitochondrial apoptotic pathway was investigated by Western blotting. As shown in Figure 8, the incubation of EL-4 cells with NQs (5 μM) induced the proteolytic activation of caspases 3 and 9 and increased the level of the cleaved form of PARP in a time-dependent manner. As expected, the increase in the level of the active form of caspase 3 occurred after the proteolytic activation of caspase 9 and prior to the cleavage of PARP, showing that these events are sequential.

4. DISCUSSION

β-Lapachone, an *o*-naphthoquinone, proved to be an effective cytostatic agent against different tumor cells, such as murine leukemia, melanoma, and hepatoma cells and human leukemia, colon carcinoma, lymphoma, and glioma cells, as well as epidermoid laryngeal, ovarian, breast, lung and prostate cancer cells (Dolan et al., 1998; Frydman et al., 1997; Li et al., 1993; Li et al., 1995; Li et al., 1999b; Pardee et al., 2002; Planchon

et al., 1999; Samali et al., 1999). Based on these effects, the clinical use of β-lapachone has been suggested (Pardee et al., 2002), and the synthesis of a number new of *o*-naphthoquinones, such as NQs, has been pursued (Ferreira et al., 2011). The data presented in this paper demonstrate that NQs induce the intrinsic apoptotic pathway in a manner associated with a significant ROS increase in the EL-4 cell line.

Our results show that NQs decrease cell proliferation in a concentration-dependent manner. Moreover, NQs decreased cell viability in a time-dependent manner at the same concentration that interfered with cell proliferation, demonstrating that at least part of the observed effect on proliferation was actually due to the compounds' ability to induce cell death. The data show that the type of cell death induced by treatment with *o*-naphthoquinones depends on the target cell type, time, and drug dose (Li et al., 1999b; Pardee et al., 2002). The results of the present study confirm that NQs (5 μM) can induce apoptosis in the EL-4 cell line. This finding was supported by three methods: Hoechst 33258 staining, double staining with AO/EB and double staining with annexin V-FITC and PI. We observed apoptotic features such as chromatin condensation and alterations in the structure, size, and shape of the nucleus that are characteristic of apoptosis. A time-course analysis of the cellular biochemistry showed that the population of apoptotic cells analyzed by double staining formed predominantly after a short incubation period (3.5 h) with NQs. After prolonged incubation, a higher percentage of late apoptotic cells was noted.

The most prominent chemical feature of quinones (Qs) is their ability to undergo redox cycling to generate ROS, and thus, damage to tumor cell results from the ability of Qs to undergo enzymatic reduction to the semiquinone radical ($Q^{\bullet}$) (reactions 1, 2 and 3) (Inbaraj and Chignell, 2004; Kalyanaraman et al., 1991; Seshadri et al., 2011). Under aerobic conditions, the semiquinone radical participates in redox cycling to generate the superoxide anion radical $O_2^{\bullet -}$ and H_2O_2 (reactions 4-7). Increased ROS may cause damage to DNA, lipids, and proteins, leading to apoptosis (Boveris et al., 1978b; Halliwell and Aruoma, 1991; Valko et al., 2007). We demonstrated that NQs (5 mM) generated semiquinone radicals in EL-4 cells. The detection of semiquinone radicals formed by enzymatic reduction requires very high concentrations of the quinone due to the relatively slow rates of formation of the semiquinone by the enzyme and their much faster rates of decay (reaction 8) (Butler et al., 1987; Cadenas, 1995). The redox

activation of these NQs by intracellular reductases in EL-4 cells and the intracellular localization of the semiquinone and the derived oxygen radicals do not rule out plasma membrane effects originating from this process (Kumar et al., 2002).

$$Q + NADPH \xrightarrow{NADPH:citP450reductase} Q^{\bullet} + NADP^{+} + H^{+} \quad (1)$$

$$Q + NADH \xrightarrow{NADH:dehydrogenase} Q^{\bullet} + NAD^{+} + H^{+} \quad (2)$$

$$Q + 2NAD(P)H \xrightarrow{NQO1} 2NAD(P)^{+} + QH_2 \quad (3)$$

$$H^{+} + QH^{-} + O_2 \rightleftharpoons Q^{\bullet} + O_2^{\bullet -} + 2H^{+} \quad (4)$$

$$H^{+} + QH^{-} + O_2^{\bullet -} \rightleftharpoons Q^{\bullet} + H_2O_2 \quad (5)$$

$$Q^{\bullet} + O_2 \rightleftharpoons Q + O_2^{\bullet -} \quad (6)$$

$$2O_2^{\bullet -} + 2H^{+} \xrightarrow{SOD} H_2O_2 + O_2 \quad (7)$$

$$Q^{\bullet -} + Q^{\bullet -} \rightleftharpoons Q + Q^{2-} \quad (8)$$

Our study confirmed that NQs produce ROS in the EL-4 cell line. It was observed that ROS production measured by the DCFDA method is a time-dependent effect, reaching maximum values at 30 min of incubation. At longer times, we observed a decrease in the intracellular content of ROS (data not shown). This decrease can be attributed to the termination reactions that involve free radicals, as well as to the dissemination of these species to the extracellular space, making them undetectable by flow cytometry. In close agreement with our results, several studies using other *o*-naphthoquinones, such as β-lapachone-based 1,2,3-triazoles, suggest that the induction of apoptosis is associated with ROS production in different human cell lines from leukemias, melanomas, colon tissue and central nervous system tissue (da Silva et al., 2011). In addition, ROS formation and apoptosis have also been observed in response to treatment with 1,2-naphthoquinone in human MCF-7 breast cancer cells (Lin et al., 2007), with 7-hydroxy-β-lapachone in human cell lines from breast, cervix, lung and colon (Rios-Luci et al.,

2012) and with 3'-nitro-3-phenylamino nor-β-lapachone against HL-60 cell line (Araujo et al., 2012).

Oxidized glutathione (GSSG) accumulates in cells under conditions of oxidative stress, and the GSH/GSSG ratio is a good indicator of this process (Nogueira et al., 2004). Numerous studies demonstrate that there is a close correlation between the increase in ROS production and the decrease in the intracellular GSH levels (Armstrong et al., 2002). A decrease in the GSH/GSSG ratio with NQ treatment is indicative of oxidative stress in treated EL-4 cells.

N-Acetyl-cysteine (NAC) protects cells by promoting GSH synthesis and scavenging ROS (Zafarullah et al., 2003). The addition of this precursor to the cell cultures resulted in a reversal of NQs-induced ROS increasing, GSH/GSSG ratio decrease and cell proliferation inhibition, confirming that the mechanism of action of these drugs is based on the generation of ROS. It should be noted that it is essential to pre-incubate EL-4 cells with NAC to observe significant differences in the proliferative response with respect to cells treated with NQs alone. This behavior may be related to the time required for the synthesis of GSH from NAC or to the fact that the cells previously required a higher concentration of GSH to compensate for the increase in ROS production caused by the action of NQs.

The alteration of the GSH/GSSG redox couple induced by ROS governs the cell death pathways by inducing the opening of the mitochondrial permeability transition pore (PTP), leading to the collapse of the mitochondrial membrane potential (MMP) and the release of proapoptotic factors (Coppola and Ghibelli, 2000; Hampton et al., 1998; Kroemer et al., 2007). Several studies have indicated that mitochondrial dysfunction and cellular energy depletion play a major role in the mechanism of cell killing by quinones with differing structures and chemical reactivities (Pritsos and Vimalachandra, 1995; Tudor et al., 2003). In accordance with these studies, a decrease in the MMP was observed in the NQ-treated EL-4 cells. These mitochondrial alterations then induce the downstream apoptotic events such as cytochrome c release and apoptosome complex formation involving Apaf-1 and procaspase 9, resulting in caspase 9 activation. Our results show that NQ treatment induces the proteolytic cleavage of procaspase 9 in EL-4 cells, generating a 37 kDa fragment that corresponds to the active form of the enzyme. Procaspase 3 is a target of caspase 9, whose action releases an 18 kDa fragment with

catalytic activity. In this context, our results also suggest that apoptosis induced by NQs is dependent on caspase 3, a conclusion that is supported by the evidence that the DNA repair enzyme PARP-1 is cleaved. We found a time-dependent increase in the cleavage of PARP that was downstream of caspase 9 and caspase 3, indicative of a cascade of sequential events. These results indicate that the NQs induce apoptosis through the activation of the intrinsic or mitochondrial pathway, as has been demonstrated for β-lapachone in human cancer cell lines derived from prostate (Weller et al., 1997), malignant glioma (Planchon et al., 1995), leukemia (Woo et al., 2006), colon (Wuerzberger et al., 1998) (Choi et al., 2003), breast (Li et al., 1999a), ovarian (Lai et al., 1998), hepatoma (Li et al., 2000), and pancreatic tumors (Ough et al., 2005) and for other *o*-naphthoquinones at concentrations in the range of 1-10 μM (IC_{50}) (D'Anneo et al., 2010; Tudor et al., 2003). However, we can not exclude the possibility that the extrinsic apoptotic pathway also contribute to NQs-induced apoptosis in EL-4 cells.

It is worth mentioning that no significant difference was found between NQs in any of the analyzed parameters in the EL-4 cell line. This result can be easily explained by the structural characteristics of the studied naphthoquinones. They do not differ in terms of their electronic, steric and lipophilic properties, with the only structural difference being in the position of a methyl group or the absence thereof. However, NQs were more active than β-lapachone against EL-4 cell line. Thus, these new derivatives present a promising profile for further experimental investigations.

Finally, our results indicate that novel NQs induce redox cycling through the production of ROS in EL-4 cells. This mechanism could be responsible for the inhibition of cell proliferation and for the cell death by apoptosis. The evaluation of the effectiveness of drugs with cytotoxic effects against tumor lines and the analysis of the mechanisms of action involved could be helpful in the treatment of cancer. In addition, the inhibitory effects of NQs in *in vivo* tumor models in mice may constitute an important part of the study of potential antitumoral drugs.

Acknowledgements

María Rosa Gonzalez Murano, María Alejandra Paulazo, Sara del Valle, María Cristina Lincon and María Alejandra Verón lent excellent technical assistance.

This research was supported by grants from the CONICET (PIP 6100 and PIP 112-200801-0275) to M.D. and G.C. respectively, and from the FAPERJ to V.F.F.

M.L.B., G.C., M.G. and M.D. are Members of the Research Career of CONICET, Argentina.

REFERENCES

Araujo, A.J., de Souza, A.A., da Silva Junior, E.N., Marinho-Filho, J.D., de Moura, M.A., Rocha, D.D., Vasconcellos, M.C., Costa, C.O., Pessoa, C., de Moraes, M.O., Ferreira, V.F., de Abreu, F.C., Pinto, A.V., Montenegro, R.C., Costa-Lotufo, L.V., Goulart, M.O., 2012. Growth inhibitory effects of 3'-nitro-3-phenylamino nor-beta-lapachone against HL-60: a redox-dependent mechanism. Toxicol In Vitro 26, 585-594.

Armstrong, J.S., Steinauer, K.K., Hornung, B., Irish, J.M., Lecane, P., Birrell, G.W., Peehl, D.M., Knox, S.J., 2002. Role of glutathione depletion and reactive oxygen species generation in apoptotic signaling in a human B lymphoma cell line. Cell Death Differ 9, 252-263.

Asche, C., 2005. Antitumour quinones. Mini Rev Med Chem 5, 449-467.

Pritsos, C.A., Vimalachandra, B., 1995. Mitochondrial dysfunction and ATP depletion in mitomycin C treated mice. Proc Am Assoc Cancer Res 36, 352-356.

Barreiro Arcos, M.L., Gorelik, G., Klecha, A., Goren, N., Cerquetti, C., Cremaschi, G.A., 2003. Inducible nitric oxide synthase-mediated proliferation of a T lymphoma cell line. Nitric Oxide 8, 111-118.

Bolton, J.L., Trush, M.A., Penning, T.M., Dryhurst, G., Monks, T.J., 2000. Role of quinones in toxicology. Chem Res Toxicol 13, 135-160.

Boveris, A., Docampo, R., Turrens, J.F., Stoppani, A.O., 1978a. Effect of beta-lapachone on superoxide anion and hydrogen peroxide production in Trypanosoma cruzi. Biochem J 175, 431-439.

Boveris, A., Stoppani, A.O., Docampo, R., Cruz, F.S., 1978b. Superoxide anion production and trypanocidal action of naphthoquinones on Trypanosoma cruzi. Comp Biochem Physiol C 61 C, 327-329.

Brunmark, A., Cadenas, E., 1989. Redox and addition chemistry of quinoid compounds and its biological implications. Free Radic Biol Med 7, 435-477.

Butler, J., Hoey, B.M., Lea, J.S., 1987. The reduction of anti-tumour diaziridinyl benzoquinones. Biochim Biophys Acta 925, 144-149.

Cadenas, E., 1995. Antioxidant and prooxidant functions of DT-diaphorase in quinone metabolism. Biochem Pharmacol 49, 127-140.

Coligan, J.E., Kruisbeek, A.M., Margulies, D.H., Shevach, E.M., Strober, W., 1995. Current Protocols in Immunology, In: Coico, R. (Ed.), Related isolation procedures and functional assays. John Wiley & Sons, Inc., p. 3.17.11.

Coppola, S., Ghibelli, L., 2000. GSH extrusion and and the mitochondrial pathway of apoptotic signalling. Biochem Soc Trans 28, 56-61.

Costantino, L., Barlocco, D., 2006. Privileged structures as leads in medicinal chemistry. Curr Med Chem 13, 65-85.

Choi, B.T., Cheong, J., Choi, Y.H., 2003. beta-Lapachone-induced apoptosis is associated with activation of caspase-3 and inactivation of NF-kappaB in human colon cancer HCT-116 cells. Anticancer Drugs 14, 845-850.

D'Anneo, A., Augello, G., Santulli, A., Giuliano, M., di Fiore, R., Messina, C., Tesoriere, G., Vento, R., 2010. Paclitaxel and beta-lapachone synergistically induce apoptosis in human retinoblastoma Y79 cells by downregulating the levels of phospho-Akt. J Cell Physiol 222, 433-443.

da Silva, E.N., Jr., Cavalcanti, B.C., Guimaraes, T.T., Pinto Mdo, C., Cabral, I.O., Pessoa, C., Costa-Lotufo, L.V., de Moraes, M.O., de Andrade, C.K., Dos Santos, M.R., de Simone, C.A., Goulart, M.O., Pinto, A.V., 2011. Synthesis and evaluation of quinonoid compounds against tumor cell lines. Eur J Med Chem 46, 399-410.

de Witte, N.V., Stoppani, A.O., Dubin, M., 2004. 2-Phenyl-beta-lapachone can affect mitochondrial function by redox cycling mediated oxidation. Arch Biochem Biophys 432, 129-135.

Dolan, M.E., Frydman, B., Thompson, C.B., Diamond, A.M., Garbiras, B.J., Safa, A.R., Beck, W.T., Marton, L.J., 1998. Effects of 1,2-naphthoquinones on human tumor cell growth and lack of cross-resistance with other anticancer agents. Anticancer Drugs 9, 437-448.

Donadelli, M., Dalla Pozza, E., Costanzo, C., Scupoli, M.T., Piacentini, P., Scarpa, A., Palmieri, M., 2006. Increased stability of P21(WAF1/CIP1) mRNA is required for ROS/ERK-dependent pancreatic adenocarcinoma cell growth inhibition by pyrrolidine dithiocarbamate. Biochim Biophys Acta 1763, 917-926.

dos Santos, E.V., Carneiro, J.W., Ferreira, V.F., 2004. Quantitative structure-activity relationship in aziridinyl-1,4-naphthoquinone antimalarials: study of theoretical correlations by the PM3 method. Bioorg Med Chem 12, 87-93.

Droge, W., 2002. Free radicals in the physiological control of cell function. Physiol Rev 82, 47-95.

Edmonson, J.H., Ryan, L.M., Blum, R.H., Brooks, J.S., Shiraki, M., Frytak, S., Parkinson, D.R., 1993. Randomized comparison of doxorubicin alone versus ifosfamide plus doxorubicin or mitomycin, doxorubicin, and cisplatin against advanced soft tissue sarcomas. J Clin Oncol 11, 1269-1275.

Elingold, I., Taboas, M.I., Casanova, M.B., Galleano, M., Silva, R.S., Menna-Barreto, R.F., Ventura Pinto, A., de Castro, S.L., Costa, L.E., Dubin, M., 2009. Mechanism of action of novel naphthofuranquinones on rat liver microsomal peroxidation. Chem Biol Interact 182, 213-219.

Fernandez Villamil, S., Stoppani, A.O., Dubin, M., 2004. Redox cycling of beta-lapachone and structural analogues in microsomal and cytosol liver preparations. Methods Enzymol 378, 67-87.

Fernandez Villamil, S.H., Carrizo, P.H., Di Rosso, M.E., Molina Portela, M.P., Dubin, M., 2012. The metabolism of 9-chloro-beta-lapachone and its effects in isolated hepatocytes. The involvement of NAD(P)H:quinone oxidoreductase 1 (NQO1). Chem Biol Interact 200, 84-91.

Ferreira, S.B., Salomao, K., de Carvalho da Silva, F., Pinto, A.V., Kaiser, C.R., Pinto, A.C., Ferreira, V.F., de Castro, S.L., 2011. Synthesis and anti-Trypanosoma cruzi activity of beta-lapachone analogues. Eur J Med Chem 46, 3071-3077.

Frydman, B., Marton, L.J., Sun, J.S., Neder, K., Witiak, D.T., Liu, A.A., Wang, H.M., Mao, Y., Wu, H.Y., Sanders, M.M., Liu, L.F., 1997. Induction of DNA topoisomerase II-mediated DNA cleavage by beta-lapachone and related naphthoquinones. Cancer Res 57, 620-627.

Gago-Martinez, A., Nogueiras, M.J., Rellan, S., Prado, J., Alpendurada, M.F., Vetter, W., 2004. Optimization of solid-phase microextraction for the gas chromatography/mass spectrometry analysis of persistent organic pollutants. J AOAC Int 87, 1021-1027.

Goijman, S.G., Stoppani, A.O., 1985. Effects of beta-lapachone, a peroxide-generating quinone, on macromolecule synthesis and degradation in Trypanosoma cruzi. Arch Biochem Biophys 240, 273-280.

Griffith, O.W., 1980. Determination of glutathione and glutathione disulfide using glutathione reductase and 2-vinylpyridine. Anal Biochem 106, 207-212.

Gross, C.L., Innace, J.K., Hovatter, R.C., Meier, H.L., Smith, W.J., 1993. Biochemical manipulation of intracellular glutathione levels influences cytotoxicity to isolated human lymphocytes by sulfur mustard. Cell Biol Toxicol 9, 259-267.

Halliwell, B., Aruoma, O.I., 1991. DNA damage by oxygen-derived species. Its mechanism and measurement in mammalian systems. FEBS Lett 281, 9-19.

Hampton, M.B., Fadeel, B., Orrenius, S., 1998. Redox regulation of the caspases during apoptosis. Ann N Y Acad Sci 854, 328-335.

Hillard, E.A., de Abreu, F.C., Ferreira, D.C., Jaouen, G., Goulart, M.O., Amatore, C., 2008. Electrochemical parameters and techniques in drug development, with an emphasis on quinones and related compounds. Chem Commun (Camb), 2612-2628.

Inbaraj, J.J., Chignell, C.F., 2004. Cytotoxic action of juglone and plumbagin: a mechanistic study using HaCaT keratinocytes. Chem Res Toxicol 17, 55-62.

Kalyanaraman, B., Morehouse, K.M., Mason, R.P., 1991. An electron paramagnetic resonance study of the interactions between the adriamycin semiquinone, hydrogen peroxide, iron-chelators, and radical scavengers. Arch Biochem Biophys 286, 164-170.

Kongkathip, N., Kongkathip, B., Siripong, P., Sangma, C., Luangkamin, S., Niyomdecha, M., Pattanapa, S., Piyaviriyagul, S., Kongsaeree, P., 2003. Potent antitumor activity of synthetic 1,2-Naphthoquinones and 1,4-Naphthoquinones. Bioorg Med Chem 11, 3179-3191.

Kroemer, G., Galluzzi, L., Brenner, C., 2007. Mitochondrial membrane permeabilization in cell death. Physiol Rev 87, 99-163.

Kumar, S., Villinger, F., Oakley, M., Aguiar, J.C., Jones, T.R., Hedstrom, R.C., Gowda, K., Chute, J., Stowers, A., Kaslow, D.C., Thomas, E.K., Tine, J., Klinman, D., Hoffman, S.L., Weiss, W.W., 2002. A DNA vaccine encoding the 42 kDa C-terminus of merozoite surface protein 1 of Plasmodium falciparum induces antibody, interferon-gamma and cytotoxic T cell responses in rhesus monkeys: immuno-stimulatory effects of granulocyte macrophage-colony stimulating factor. Immunol Lett 81, 13-24.

Kumar, S.G., Narayana, K., Bairy, K.L., D'Souza, U.J., Samuel, V.P., Gopalakrishna, K., 2006. Dacarbazine induces genotoxic and cytotoxic germ cell damage with concomitant decrease in testosterone and increase in lactate dehydrogenase concentration in the testis. Mutat Res 607, 240-252.

Lai, C.C., Liu, T.J., Ho, L.K., Don, M.J., Chau, Y.P., 1998. beta-Lapachone induced cell death in human hepatoma (HepA2) cells. Histol Histopathol 13, 89-97.

LeBel, C.P., Ischiropoulos, H., Bondy, S.C., 1992. Evaluation of the probe 2',7'-dichlorofluorescin as an indicator of reactive oxygen species formation and oxidative stress. Chem Res Toxicol 5, 227-231.

Li, C.J., Averboukh, L., Pardee, A.B., 1993. beta-Lapachone, a novel DNA topoisomerase I inhibitor with a mode of action different from camptothecin. J Biol Chem 268, 22463-22468.

Li, C.J., Li, Y.Z., Pinto, A.V., Pardee, A.B., 1999a. Potent inhibition of tumor survival in vivo by beta-lapachone plus taxol: combining drugs imposes different artificial checkpoints. Proc Natl Acad Sci U S A 96, 13369-13374.

Li, C.J., Wang, C., Pardee, A.B., 1995. Induction of apoptosis by beta-lapachone in human prostate cancer cells. Cancer Res 55, 3712-3715.

Li, Y., Li, C.J., Yu, D., Pardee, A.B., 2000. Potent induction of apoptosis by beta-lapachone in human multiple myeloma cell lines and patient cells. Mol Med 6, 1008-1015.

Li, Y.Z., Li, C.J., Pinto, A.V., Pardee, A.B., 1999b. Release of mitochondrial cytochrome C in both apoptosis and necrosis induced by beta-lapachone in human carcinoma cells. Mol Med 5, 232-239.

Lin, C.H., Huang, C.C., Wang, T.W., Wang, Y.J., Lin, P.H., 2007. Disparity in the induction of glutathione depletion, ROS formation, poly(ADP-ribose) polymerase-1

activation, and apoptosis by quinonoid derivatives of naphthalene in human cultured cells. Chem Biol Interact 165, 200-210.
Lopes, J.N., Cruz, F.S., Docampo, R., Vasconcellos, M.E., Sampaio, M.C., Pinto, A.V., Gilbert, B., 1978. In vitro and in vivo evaluation of the toxicity of 1,4-naphthoquinone and 1,2-naphthoquinone derivatives against Trypanosoma cruzi. Ann Trop Med Parasitol 72, 523-531.
Molina Portela, M.P., Fernandez Villamil, S.H., Perissinotti, L.J., Stoppani, A.O., 1996. Redox cycling of o-naphthoquinones in trypanosomatids. Superoxide and hydrogen peroxide production. Biochem Pharmacol 52, 1875-1882.
Molina Portela, M.P., Stoppani, A.O., 1996. Redox cycling of beta-lapachone and related o-naphthoquinones in the presence of dihydrolipoamide and oxygen. Biochem Pharmacol 51, 275-283.
Nogueira, C.W., Zeni, G., Rocha, J.B., 2004. Organoselenium and organotellurium compounds: toxicology and pharmacology. Chem Rev 104, 6255-6285.
Ough, M., Lewis, A., Bey, E.A., Gao, J., Ritchie, J.M., Bornmann, W., Boothman, D.A., Oberley, L.W., Cullen, J.J., 2005. Efficacy of beta-lapachone in pancreatic cancer treatment: exploiting the novel, therapeutic target NQO1. Cancer Biol Ther 4, 95-102.
Pardee, A.B., Li, Y.Z., Li, C.J., 2002. Cancer therapy with beta-lapachone. Curr Cancer Drug Targets 2, 227-242.
Planchon, S.M., Wuerzberger-Davis, S.M., Pink, J.J., Robertson, K.A., Bornmann, W.G., Boothman, D.A., 1999. Bcl-2 protects against beta-lapachone-mediated caspase 3 activation and apoptosis in human myeloid leukemia (HL-60) cells. Oncol Rep 6, 485-492.
Planchon, S.M., Wuerzberger, S., Frydman, B., Witiak, D.T., Hutson, P., Church, D.R., Wilding, G., Boothman, D.A., 1995. Beta-lapachone-mediated apoptosis in human promyelocytic leukemia (HL-60) and human prostate cancer cells: a p53-independent response. Cancer Res 55, 3706-3711.
Rios-Luci, C., Bonifazi, E.L., Leon, L.G., Montero, J.C., Burton, G., Pandiella, A., Misico, R.I., Padron, J.M., 2012. beta-Lapachone analogs with enhanced antiproliferative activity. Eur J Med Chem 53, 264-274.
Samali, A., Nordgren, H., Zhivotovsky, B., Peterson, E., Orrenius, S., 1999. A comparative study of apoptosis and necrosis in HepG2 cells: oxidant-induced caspase inactivation leads to necrosis. Biochem Biophys Res Commun 255, 6-11.
Seshadri, P., Rajaram, A., Rajaram, R., 2011. Plumbagin and juglone induce caspase-3-dependent apoptosis involving the mitochondria through ROS generation in human peripheral blood lymphocytes. Free Radic Biol Med 51, 2090-2107.
Thor, H., Smith, M.T., Hartzell, P., Bellomo, G., Jewell, S.A., Orrenius, S., 1982. The metabolism of menadione (2-methyl-1,4-naphthoquinone) by isolated hepatocytes. A study of the implications of oxidative stress in intact cells. J Biol Chem 257, 12419-12425.
Tudor, G., Gutierrez, P., Aguilera-Gutierrez, A., Sausville, E.A., 2003. Cytotoxicity and apoptosis of benzoquinones: redox cycling, cytochrome c release, and BAD protein expression. Biochem Pharmacol 65, 1061-1075.
Valko, M., Leibfritz, D., Moncol, J., Cronin, M.T., Mazur, M., Telser, J., 2007. Free radicals and antioxidants in normal physiological functions and human disease. Int J Biochem Cell Biol 39, 44-84.
Vermes, I., Haanen, C., Steffens-Nakken, H., Reutelingsperger, C., 1995. A novel assay for apoptosis. Flow cytometric detection of phosphatidylserine expression on early apoptotic cells using fluorescein labelled Annexin V. J Immunol Methods 184, 39-51.

Walsh, G.M., Dewson, G., Wardlaw, A.J., Levi-Schaffer, F., Moqbel, R., 1998. A comparative study of different methods for the assessment of apoptosis and necrosis in human eosinophils. J Immunol Methods 217, 153-163.

Weller, M., Winter, S., Schmidt, C., Esser, P., Fontana, A., Dichgans, J., Groscurth, P., 1997. Topoisomerase-I inhibitors for human malignant glioma: differential modulation of p53, p21, bax and bcl-2 expression and of CD95-mediated apoptosis by camptothecin and beta-lapachone. Int J Cancer 73, 707-714.

Woo, H.J., Park, K.Y., Rhu, C.H., Lee, W.H., Choi, B.T., Kim, G.Y., Park, Y.M., Choi, Y.H., 2006. Beta-lapachone, a quinone isolated from Tabebuia avellanedae, induces apoptosis in HepG2 hepatoma cell line through induction of Bax and activation of caspase. J Med Food 9, 161-168.

Wuerzberger, S.M., Pink, J.J., Planchon, S.M., Byers, K.L., Bornmann, W.G., Boothman, D.A., 1998. Induction of apoptosis in MCF-7:WS8 breast cancer cells by beta-lapachone. Cancer Res 58, 1876-1885.

Xu, H.L., Yu, X.F., Qu, S.C., Qu, X.R., Jiang, Y.F., Sui da, Y., 2012. Juglone, from Juglans mandshruica Maxim, inhibits growth and induces apoptosis in human leukemia cell HL-60 through a reactive oxygen species-dependent mechanism. Food Chem Toxicol 50, 590-596.

Xu, H.L., Yu, X.F., Qu, S.C., Zhang, R., Qu, X.R., Chen, Y.P., Ma, X.Y., Sui, D.Y., 2010. Anti-proliferative effect of Juglone from Juglans mandshurica Maxim on human leukemia cell HL-60 by inducing apoptosis through the mitochondria-dependent pathway. Eur J Pharmacol 645, 14-22.

Zafarullah, M., Li, W.Q., Sylvester, J., Ahmad, M., 2003. Molecular mechanisms of N-acetylcysteine actions. Cell Mol Life Sci 60, 6-20.

Figure captions

Figure 1: Chemical structure of NQs used in this study. NQ1: 2-phenyl-3,4-dihydro-2*H*-benzo[*h*]chromene-5,6-dione, NQ3: 2-p-tolyl-3,4-dihydro-2*H*-benzo[*h*]chromene-5,6-dione, NQ7: 2-methyl-2-phenyl-3,4-dihydro-2H-benzo[*h*]chromene-5,6-dione.

Figure 2: Effects of NQs on EL-4 cells proliferation and viability. EL-4 cells were cultured for 24 h in the absence or presence of increasing concentrations of NQs (● NQ1, □ NQ3 and ▲ NQ7). Cell proliferation was determined by [^{3}H]-TdR incorporation **(A)**. Values [desintegrations per minute (dpm)] are means ± SE of 4 independent experiments performed in triplicate. After incubation in the absence (control) or presence of NQs (5 M) for the indicated times, the percentage of viable cells was quantified by trypan blue exclusion dye **(B)**. Values are the means ± SE of 4 independent experiments performed in duplicate. *Significantly different from the corresponding control value ($p< 0.05$).

Figure 3: Action of NQs on cell death induction in EL-4 line. (A) EL-4 cells were cultured for 3.5 and 7 h in the absence (control) or presence of NQs (5 μM) and then labeled with acridine orange and ethidium bromide (both 100 μg/ml). Viable cells (stained in green) and apoptotic cells (stained in orange) were observed by fluorescent microscopy (1000x). Results are representative of 4 independent experiments. **(B)** EL-4 cells were incubated for 7 h in the absence (control) or presence of NQs (5 μM) and then stained with Hoechst 33258 (0.5 μg/ml) dye. Nuclear morphology was observed by fluorescent microscopy (1000x). Results showed are representative of 3 independent experiments. **(C)** EL-4 cells were cultured for 3.5 and 7 h in the absence (control) or presence of NQs (5 μM) and then labeled with propidium iodide (PI) and annexin V-FITC (annexin). Percentage of viable cells (PI-/annexin-), in early apoptosis (PI-/annexin+), delayed apoptosis (PI+/annexin+) or necrosis (PI+/annexin-) was quantified by flow cytometry. Percentages of cells corresponding to each quadrant are indicated in parentheses. Dot blot graphs showed are representative of 3 independent experiments. **(D)** Percentages of cells corresponding to each stage are shown. Results are expressed as mean ± SE from 3 independent experiments performed in triplicate. *Significantly different from corresponding control value ($p< 0.05$).

Figure 4: Electron Paramagnetic Resonance (EPR) spectrum of *o*-semi-naphthoquinones. EL-4 cells were incubated with NQs (5 mM) and NADPH (20 mM) under anaerobic conditions. *O*-seminaphthoquinones signals were obtained following the procedure described in materials and methods sections. Spectrums (A), (B) and (C) correspond to NQ1, NQ3 and NQ7, respectively. Spectrums (D) to (F) are representative of EL-4 cells incubated with NQs in absence of NADPH (D); EL-4 cells incubated with NADPH in absence of NQs (E), and NQs incubated with NADPH in absence of cells (F). The arrow indicates a small signal corresponding to the chemical, non-enzymatic reduction. Spectrum are representative of 3 independent experiments.

Figure 5: Effect of NQs on the generation of reactive oxygen species (ROS) in the EL-4 cells. EL-4 cells were cultured in the absence (control) or presence of NQs (5 μM) for the indicated times and then labeled with H2DCF-DA to quantify the ROS production by flow cytometry **(A)**. The mean fluorescence intensity (MFI) of each treatment is indicated in parenthesis. The histograms showed are representative of 3 independent experiments. **(B)** The quantification of ROS production in function of the time of treatment with NQs is shown in the bar graph. Results are expressed as mean ± SE from 3 independent experiments performed in triplicate. *Differ significantly respect to control (p 0.05).

Figure 6: Effect of NAC on the proliferation of EL-4 cell cultured with NQs. Quantification of EL-4 cells proliferation preincubated for 18 h with different concentrations of NAC and then cultured for 24 h in the presence of 2.5 μM or 5 μM of NQ1 **(A)**, NQ3 **(B)** or NQ7 **(C)**. Bars corresponding to control indicate basal values of cell proliferation in the absence (white bars) or the presence (black bars) of NAC and without NQs. A dose-response effect of NAC on NQs inhibitory actions is depicted for the two concentrations of NQs (light and dark grey bars). Results are expressed as mean ± SE from 3 independent experiments performed in triplicate. *Differ significantly from the control value ($p<0.05$).

Figure 7: Effect of NQs on mitochondrial membrane potencial. EL-4 cells were cultured for 3.5 h in the absence (control) or presence of NQs (5 M) and then labeled with rhodamine-123 (1 μM). Changes in mitochondrial membrane potential were detected by flow cytometry. The histograms shown are representative of 3 independent experiments performed in triplicate. The bar graph indicates the mean fluorescence intensity (MFI) of rhodamine-123 retained inside the mitochondria. Results are expressed as mean ± SE from 3 independent experiments performed in triplicate. *Differ significantly respect to control ($p<0.05$).

Figure 8: Caspases proteolytic activation and Poly (ADP-Ribose) Polymerase (PARP) cleavage mediated by NQs. EL-4 cells were cultured in the absence (control, C) or presence of NQs (5 μM) for the indicated times. Proteolytic activation of caspases 9 and 3 and PARP cleavage were analyzed by western blot. Specific antibodies showed bands for active caspase 9 (37 kDa), active caspase 3 (17 kDa), cleaved PARP (89 kDa) and β-actin (43 kDa). Densitometry analyses of the results are shown in the bar graphs. Values are the means ± SE of 3 independent experiments. β-actin bands were used as protein load control. *Differ significantly respect to control ($p<0.05$).

Supplemental Figure 1: Effect of NAC on the generation of reactive oxygen species (ROS) mediated by NQs in the EL-4 cells. EL-4 cells were cultured in the absence (control) or presence of NQs (5 μM) for 30 min and then labeled with H2DCF-DA to quantify the ROS production by flow cytometry. NAC (12.5 mM) was added 18 h before compounds exposure. **(A)**. The mean fluorescence intensity (MFI) of each treatment is indicated in parenthesis. The histograms showed are representative of 3 independent experiments. **(B)** The quantification of ROS production in absence or presence of NAC pre-treatment is shown in the bar graph. Results are expressed as mean ± SE from 3 independent experiments performed in triplicate. *Differ significantly respect to control (p 0.05).

Figure 1

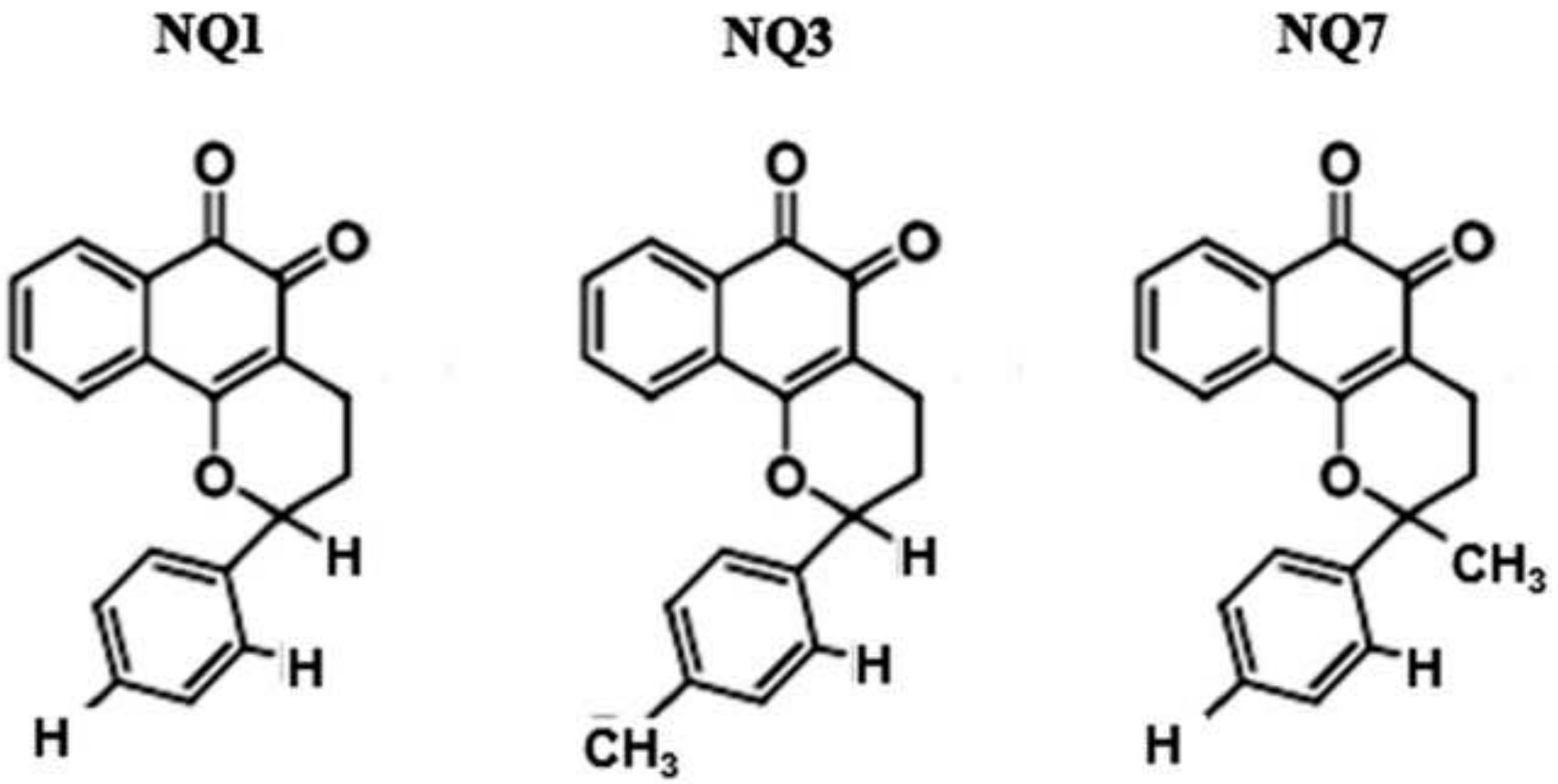

Figure 2

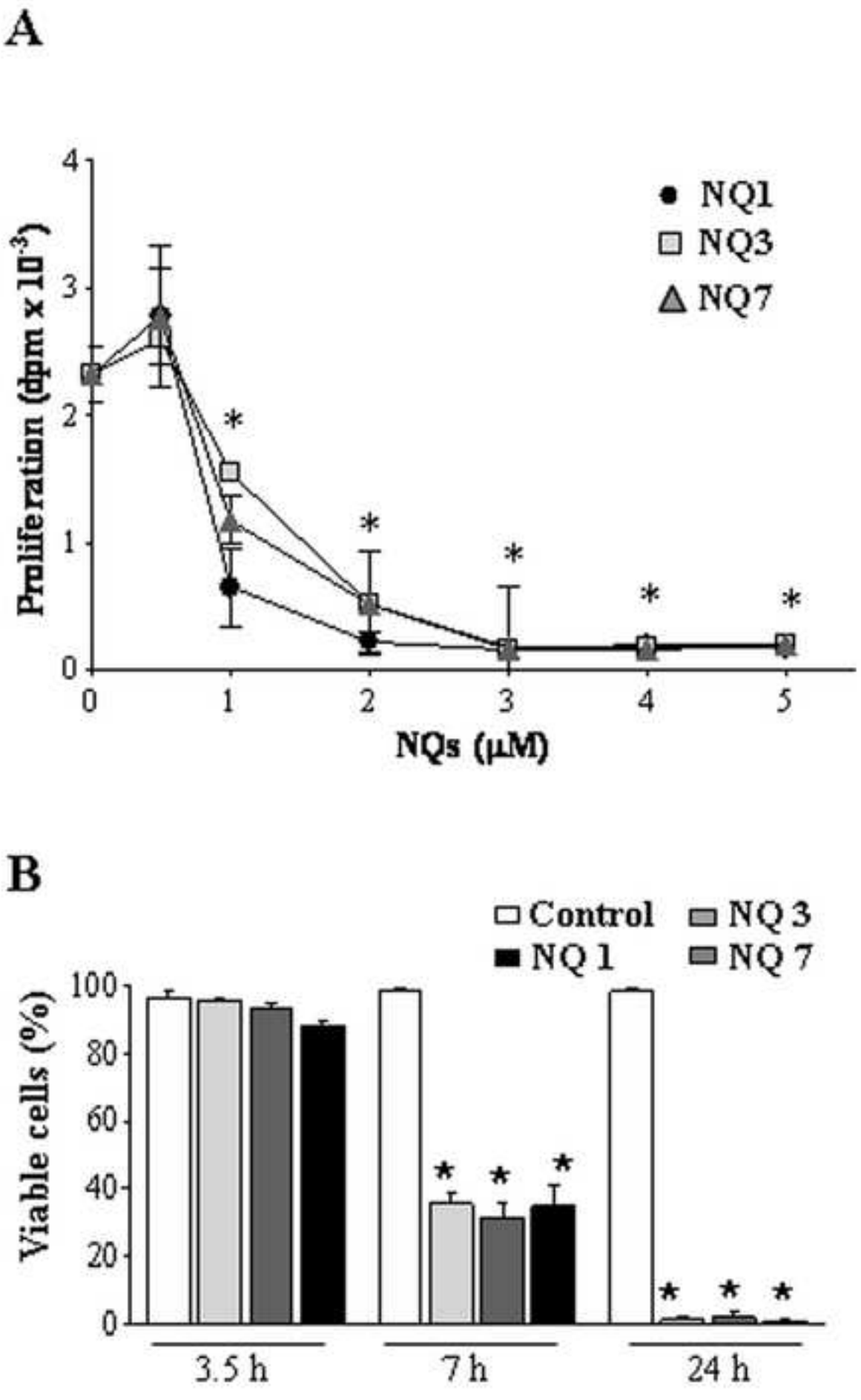

Figure 3

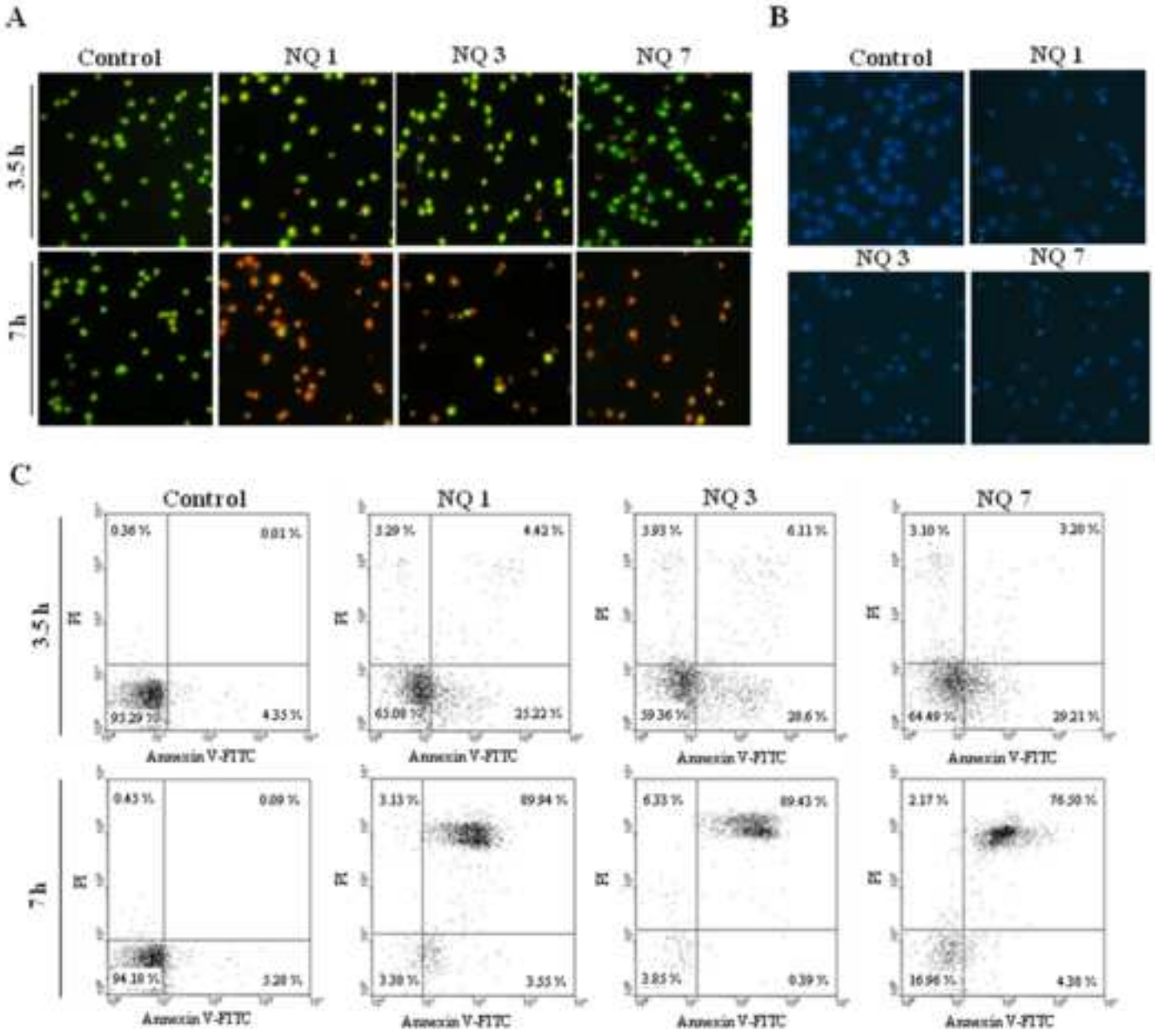

Figure 4

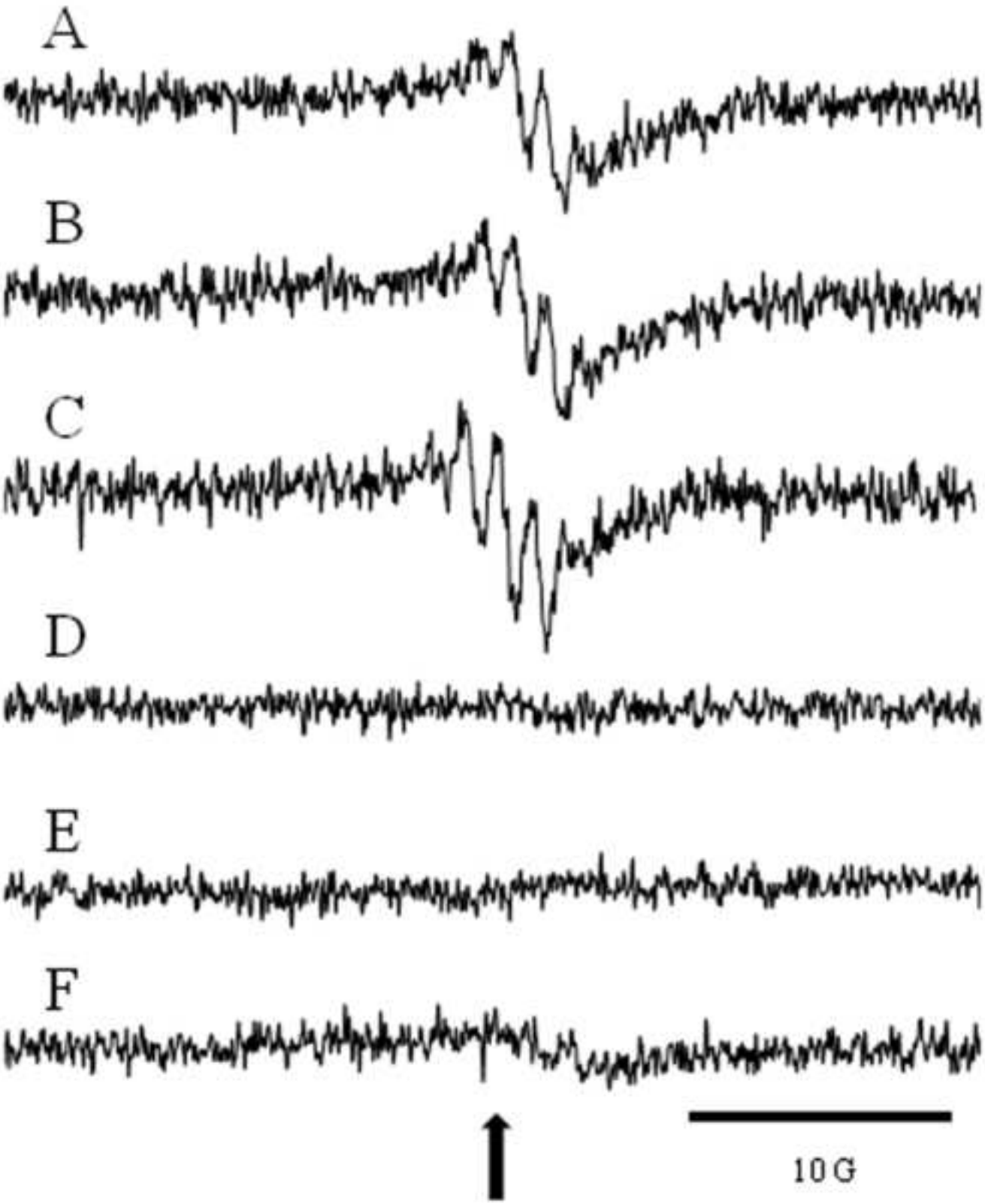

Figure 5

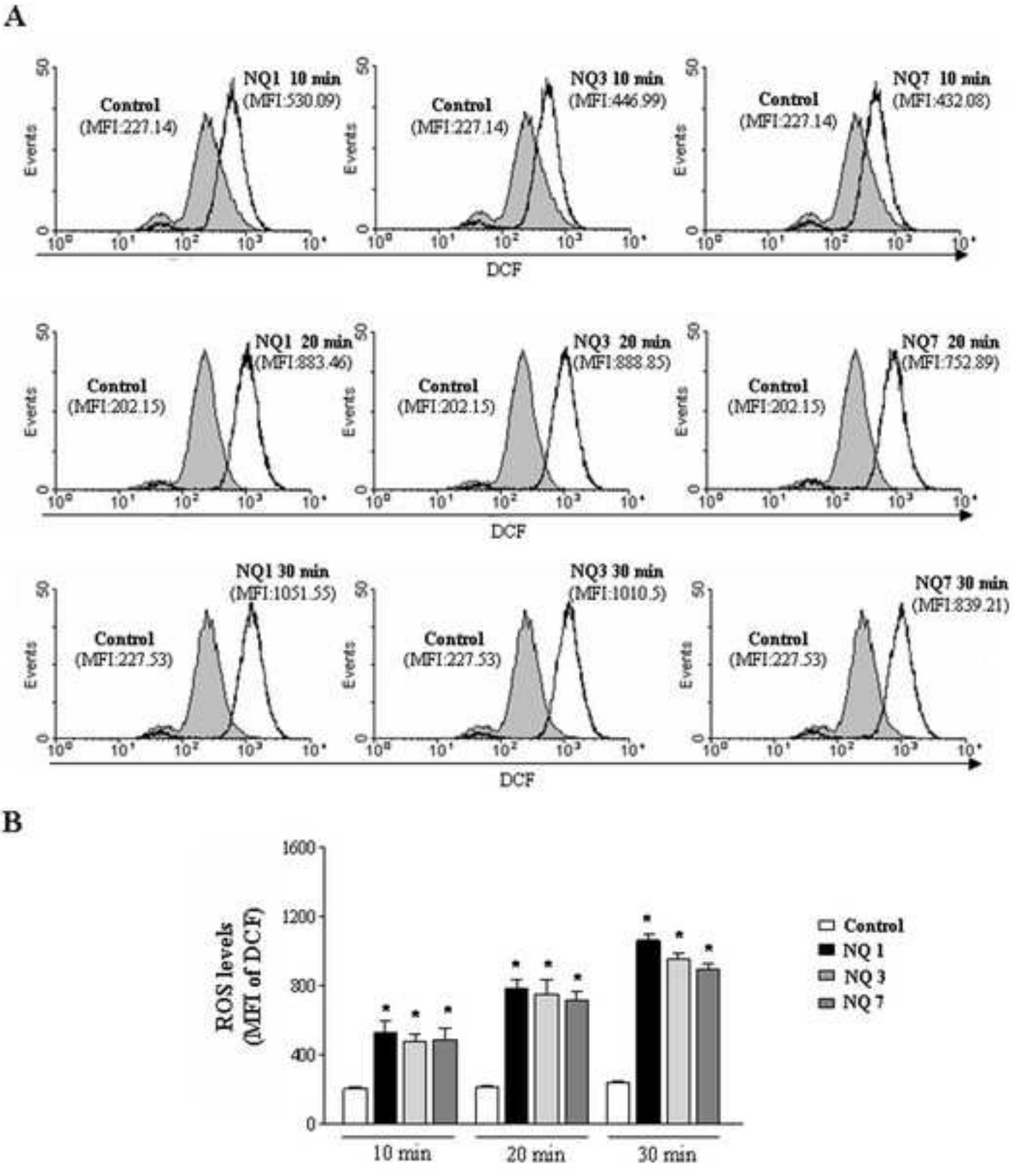

Figure 6

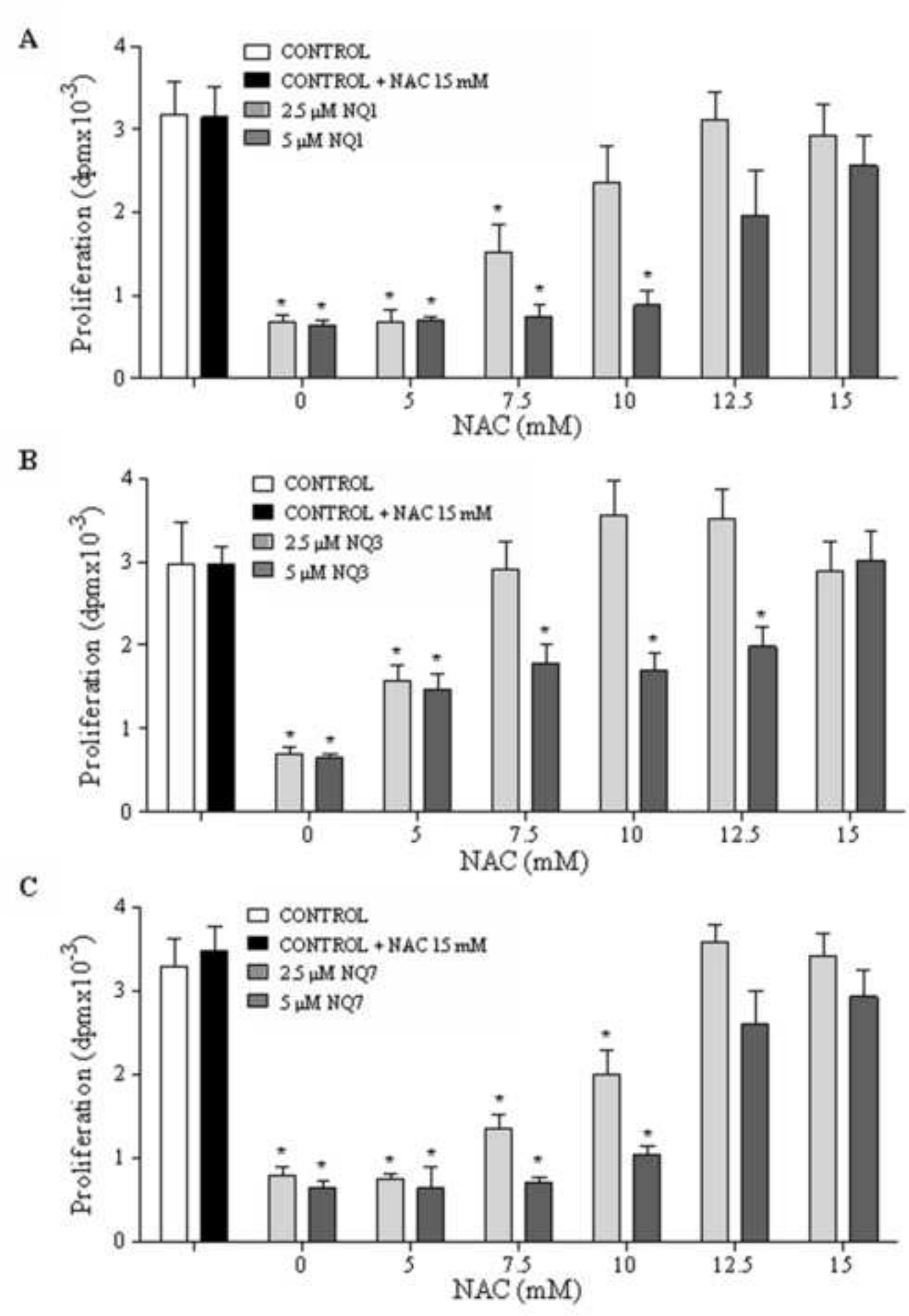

Figure 7

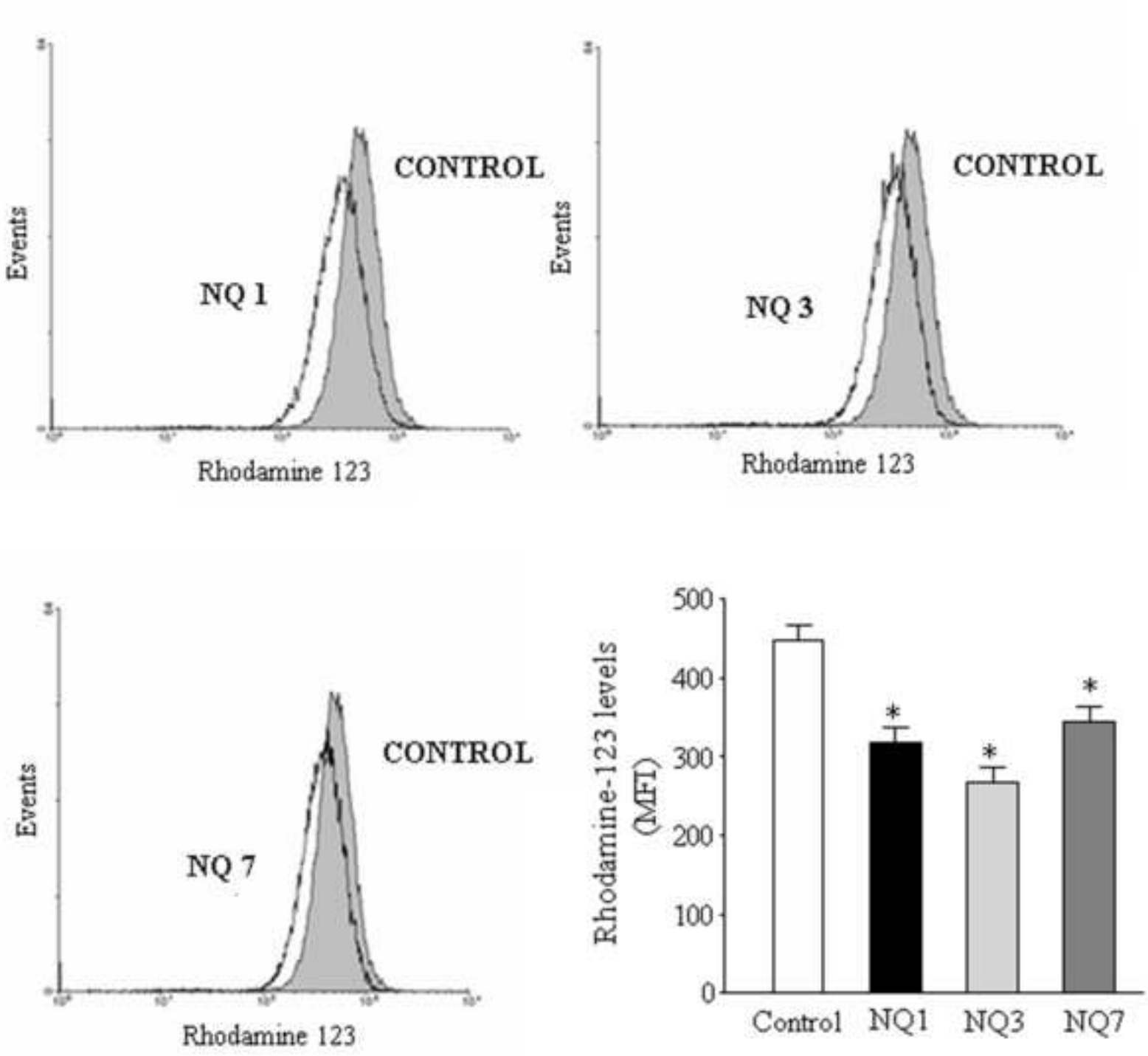

Figure 8

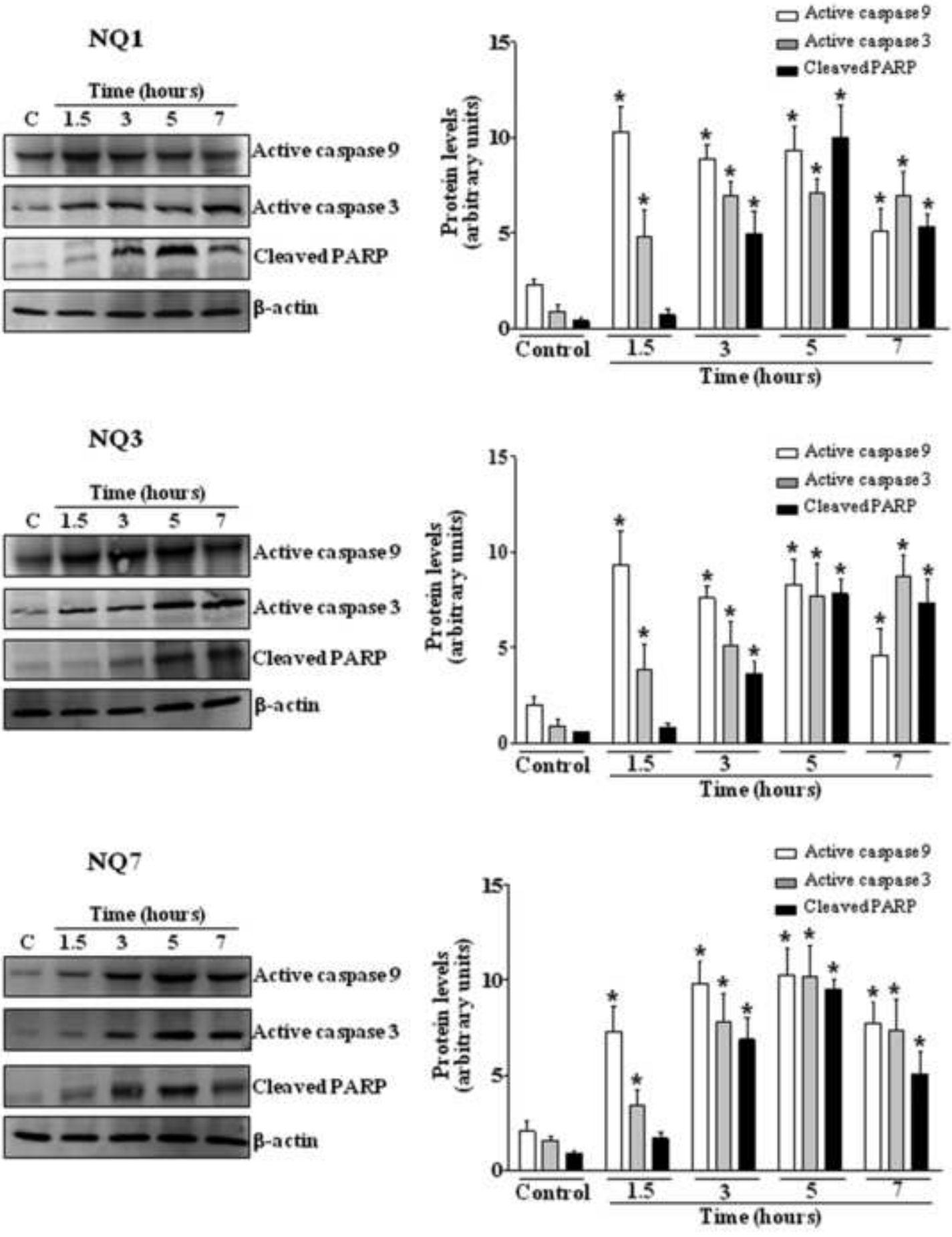

Table 1

Effect of NQs in glutathione redox state

Treatment	Total glutathione	GSH	GSSG	GSH/GSSG
	pmol/1x10^6 cells			
Control	20.57±0.85	15.95±1.2	4.62±0.35	3.45±0.15
NQ1	19.14±0.89	9.57±1.66*	9.57±0.77*	1.00±0.25*
NQ3	17.27±0.95	8.69±1.78*	8.58±0.83*	1.01±0.30*
NQ7	16.83±0.94	6.93±1.61*	9.90±0.67*	0.70±0.30*
Control+NAC	25.28±1.00*	22.23±1.36*	3.05±0.36	7.29±0.18*
NQ1+NAC	25.50±1.02*	22.38±1.28*	3.12±0.26	7.17±0.14*
NQ3+NAC	25.91±0.98*	22.66±1.31*	3.25±0.33	6.97±0.16*
NQ7+NAC	26.14±1.01*	22.61±1.30*	3.53±0.29	6.40±0.14*

EL-4 cells were cultured for 30 min in the absence (control) or the presence of NQs (5 μM). For NAC treatment, EL-4 cells were incubated with NAC (12.5 mM) for 18 h prior to incubation with NQs. GSH and GSSG content was quantified according to the procedures described in materials and methods. Each value represents the mean ± SE of three independent experiments, each in triplicate. *$p<0.05$ compared to the respective control.

Graphical abstract

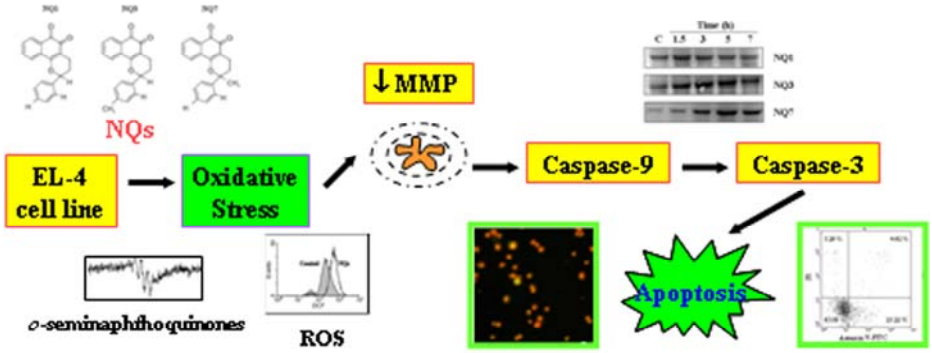

HIGHLIGHTS

- Novel β-lapachone analogs (NQs) cause cytotoxicity in EL-4 lymphoma cells.
- NQs (5 μM) can induce apoptosis in the EL-4 cell line.
- ROS generation and oxidative stress are involved in NQ-induced apoptosis.
- NQs induce apoptosis through the activation of the intrinsic pathway.